Skeletal muscle stem cells express anti-apoptotic ErbB receptors during activation from quiescence

EXPERIMENTAL CELL RESEARCH XX (2006) XXX–XXX

available at www.sciencedirect.com

ScienceDirect

www.elsevier.com/locate/yexcr

Research Article

Skeletal muscle stem cells express anti-apoptotic ErbB receptors during activation from quiescence

Jon P. Golding[a,*], Emma Calderbank[b], Terence A. Partridge[b], Jonathan R. Beauchamp[b]

[a]Department of Biological Sciences, Open University, Walton Hall, Milton Keynes, MK7 6AA, UK
[b]Muscle Cell Biology Group, Medical Research Council Clinical Sciences Centre, Faculty of Medicine, Imperial College, Hammersmith Hospital Campus, Du Cane Road, London, W12 0NN, UK

ARTICLE INFORMATION

Article Chronology:
Received 4 May 2006
Revised version received
9 October 2006
Accepted 16 October 2006

Keywords:
Muscle stem cell
Satellite cell
Apoptosis
Activation
erbB
EGFr

ABSTRACT

To be effective for tissue repair, satellite cells (the stem cells of adult muscle) must survive the initial activation from quiescence. Using an in vitro model of satellite cell activation, we show that erbB1, erbB2 and erbB3, members of the EGF receptor tyrosine kinase family, appear on satellite cells within 6 h of activation. We show that signalling via erbB2 provides an anti-apoptotic survival mechanism for satellite cells during the first 24 h, as they progress to a proliferative state. Inhibition of erbB2 signalling with AG825 reduced satellite cell numbers, concomitant with elevated caspase-8 activation and TUNEL labelling of apoptotic satellite cells. In serum-free conditions, satellite cell apoptosis could be largely prevented by a mixture of erbB1, erbB3 and erbB4 ligand growth factors, but not by neuregulin alone (erbB3/erbB4 ligand). Furthermore, using inhibitors specific to discrete intracellular signalling pathways, we identify MEK as a pro-apoptotic mediator, and the erbB-regulated factor STAT3 as an anti-apoptotic mediator during satellite cell activation. These results implicate erbB2 signalling in the preservation of a full compliment of satellite cells as they activate in the context of a damaged muscle.

Introduction

Satellite cells, a population of undifferentiated tissue-specific stem cells, comprise only about 2% of the total nuclei of normal adult skeletal muscle [1–3]. Despite this apparently small reserve of potentially proliferative cells, skeletal muscle nevertheless exhibits an astonishing regenerative capacity, with each satellite cell able to generate several thousand new myonuclei [3] on a time scale that allows total replacement of the parent myofibre within 4 days of injury [4]. Because of their fundamental role in muscle regeneration, robust mechanisms must exist to assure the survival of satellite cells within the context of a damaged muscle. Once activated from quiescence, the amplifying progeny of satellite cells (myoblasts) are sensitive to apoptotic cell death as they proliferate [5,6] and differentiate [7,8]. However, the sensitivity of satellite cells to apoptotic death during the activation process, within the first 24 h following myotrauma, has not been determined. This is a critical period during muscle regeneration, during which satellite cells undergo an important series of molecular changes prior to cell division [9–11], while at the same time having to adjust to the physiological stresses of muscle injury.

In response to myotrauma, intracellular reactive oxygen species (ROS) are generated [12–14]. ROS is a key effector of death in most cells [15] and of DNA damage in myoblasts [16], while under conditions of transient oxidative stress, human

* *Corresponding author*. Fax: +44 1908 654167.
E-mail address: j.p.golding@open.ac.uk (J.P. Golding).

0014-4827/$ – see front matter © 2006 Elsevier Inc. All rights reserved.
doi:10.1016/j.yexcr.2006.10.019

satellite cells show decreased viability and become non-proliferative [17]. Under normal conditions, catalase and glutathione transferase antioxidants expressed by quiescent satellite cells can protect against ROS [18]. However, these defence systems become overwhelmed by excessive ROS production, as occurs following injury and in various pathologies [19], highlighting the potential vulnerability of satellite cells to apoptosis following myotrauma. During the late regenerative phase, as myoblasts exit the cell cycle and differentiate, anti-apoptotic signals are transduced by two members of the erbB family of receptor tyrosine kinases: erbB1 (the EGF receptor) [20] and erbB2 [21], raising the possibility that these erbB receptors might also provide anti-apoptotic signals, during satellite cell activation.

The erbB family comprises erbB1, erbB2, erbB3 and erbB4 [22], while the metalloendopeptidase *N*-arginine dibasic convertase (NRDc) binds heparin-binding EGF-like growth factor and thereby acts as a co-receptor with erbB1 [23]. Ligand binding causes erbB receptors to dimerise and phosphorylate, with erbB2 being the preferred dimerisation partner of the other erbB receptors, although erbB2 itself has no known ligand [22]. ErbB receptors are expressed by many cell types and regulate diverse cellular functions that include proliferation, migration, cell fate decisions, differentiation and apoptosis [22,24]. In normal, undamaged skeletal muscle, erbB2, erbB3 and erbB4 receptors are exclusively localised to the neuromuscular junction (NMJ) [25,26], where they regulate the expression of acetylcholine receptors [27,28] and glucose transport within myofibres [29]. Although NRDc is highly expressed by human skeletal muscle [30], its cellular localisation has not been determined. In tissue culture models of the late phase of muscle injury, myoblasts express erbB1, erbB2 and erbB3 receptors [21,31–33], as they commit to differentiation. However, it remains unknown whether erbB receptors are expressed by satellite cells and if so, at which stage of the activation process they first appear and how their expression is regulated.

In this study, we show that satellite cells do not express any erbB receptors in the quiescent state. However, erbB1, erbB2 and erbB3 become expressed within 6 h of activation, while erbB4 and NRDc can be detected within 24 h. We demonstrate that erbB2 signalling plays an anti-apoptotic role in preserving the full complement of satellite cells during this critical phase of stem cell activation from quiescence.

Materials and methods

Animals

C57Bl/10 mice, myosin light chain 3F-nLacZ-2E (MLC-3F^{nLacZ}) mice [34] and Myf5$^{nLacZ/+}$ mice [35], aged between 6 and 8 weeks, were from breeding colonies maintained at MRC Hammersmith.

Tissue preparation and single myofibre isolation

Entire *extensor digitorum longus* (EDL) and *tibialis anterior* (TA) muscles were removed. The TAs were snap frozen for cryosectioning and the EDLs were dissociated into single muscle fibres (myofibres), as described previously [36].

Myofibre culture

Isolated myofibres were maintained as non-adherent cultures in DMEM, containing 10% horse serum (PAA Laboratories) and 0.5% chick embryo extract (ICN Flow) as described previously [36]. Myofibres were subsequently fixed with 4% paraformaldehyde in PBS (4% PAF) for 20 min prior to immunostaining.

Growth factors

Recombinant Human EGF, HB-EGF and NRG (NRG-1 β1 EGF domain) were obtained from R&D Systems.

ErbB inhibitors

The erbB1-selective inhibitor AG1478 (Calbiochem) was dissolved in DMSO and used at a 1:500 dilution to give a 10-μM working concentration (autophosphorylation: erbB1 IC_{50}=0.003μM; erbB2 IC_{50}>100 μM [37]). The erbB2-selective inhibitor AG825 (Calbiochem) was dissolved in DMSO and used at a 1:500 dilution to give a 50-μM working concentration (autophosphorylation: erbB2 IC_{50}=0.35 μM; erbB1 IC_{50}=19 μM. Substrate phosphorylation: erbB2 IC_{50}= 9.5 μM; erbB1 IC_{50}>100 μM [38]). Control cultures contained 1:500 DMSO.

Signal transduction pathway-specific inhibitors

All inhibitors were obtained from Calbiochem and were dissolved in DMSO, unless stated otherwise. The following inhibitors were used at the working concentrations shown (typically 1000-fold dilutions of the stock solution): Akt inhibitor, 10 μM (Akt IC_{50}=5 μM). U0126, MEK1/2 inhibitor, 12.5 μM (MEK1 IC_{50}=72 nM, MEK2 IC_{50}=58 nM). Jnk inhibitor II, 20 μM (Jnk-1/Jnk-2 IC_{50}=40 nM, Jnk-3 IC_{50}=90 nM). SB203580, p38MAP-K inhibitor, 2 μM (p38MAP-K IC_{50}= 600 nM). U-73122, PLCγ inhibitor, 5 μM (PLC IC_{50}=2 μM). IC_{50} values are quoted from the product data sheets. Caspase-8 competitive inhibitor I, cell-permeable, 100 nM [39]. STAT3 inhibitor, cell-permeable, 1 mM (solid dissolved directly in culture medium to working concentration, immediately prior to use) [40].

Histology

Cultured myofibres from MLC-3F^{nLacZ} mice and TA muscle cryosections from Myf5$^{nLacZ/+}$ mice were fixed in 4% PAF for 5 min. β-Galactosidase activity was visualised by incubation in 4 mM potassium ferrocyanide, 4 mM potassium ferricyanide, 2 mM $MgCl_2$, 400 μg/ml X-gal, 0.02% NP40 in PBS for 10 min at 37°C. Myofibres were then washed in PBS and processed for immunohistochemistry.

Immunostaining

Fixed myofibres were permeabilised with 0.5% Triton X-100/PBS for 10 min. Cryosections were fixed in 4% PAF for 10 min

Please cite this article as: J.P. Golding, et al., Skeletal muscle stem cells express anti-apoptotic ErbB receptors during activation from quiescence, Exp. Cell Res. (2006), doi:10.1016/j.yexcr.2006.10.019

and washed in PBS. Non-specific antibody binding was blocked by incubation in 20% goat serum in PBS for 30 min.

Rabbit anti-erbB2 (sc-284, Santa Cruz, 1:200 dilution, 1 μg/ml working conc.) and rabbit anti-erbB4 (06-572, Upstate, 1:100, 10 μg/ml working conc.) antibodies have been previously characterised on rodent skeletal muscle sections [26], while mouse anti-erbB3 antibody (Ab-5, Calbiochem, 1:100, 2 μg/ml working conc.) has been previously characterised on L6 and C2C12 rodent skeletal muscle cell lines [33]. Other primary antibodies were mouse anti-erbB1 (clone 13, BD Bioscience, 1:20, 12.5 μg/ml working concentration); mouse anti-Pax7 (Developmental Studies Hybridoma Bank, 1:10); rabbit anti-MyoD (sc-760, Santa Cruz, 1:80); mouse anti-MyoD1 (clone 5.8A, DakoCytomation, 1:80); mouse anti-myogenin (clone F5D, Developmental Studies Hybridoma Bank, 1:80); rabbit anti-NRDc (gift of Annik Prat, Institut de Recherches Cliniques de Montreal, 1:400); rat anti-BrdU (Abcam, 1:500, used as in [10]); rabbit anti-phospho(Tyr877)-erbB2 and rabbit anti-phospho (Tyr1248)-erbB2 (Cell Signalling Technology, used together at 1:50); rabbit anti-phospho(Tyr1173)-erbB1 (ab5652, Abcam, 1:100). Control mouse and rabbit IgG were used in place of primary antibodies at 10 μg/ml.

Primary antibodies were applied overnight at 4°C and then visualised by 2 h incubation with Alexa Fluor-conjugated secondary antibodies (Molecular Probes, 1:200). Where indicated, Texas Red-conjugated α-bungarotoxin (Molecular probes, 1:1000) was mixed with the secondary antibody.

Immunostaining with antibodies against phosphorylated erbBs was carried out as above, except all solutions contained 100 mM sodium orthovanadate. For de-phosphorylation controls, permeabilised myofibres were incubated with 6 U/ml alkaline phosphatase (Promega) in PBS pH8, without orthovanadate, for 2 h at 37°C before proceeding with serum blocking and primary antibodies.

Myofibres were mounted in Faramount (DakoCytomation) containing either 100 ng/ml 1,4-diazobicyclo[2,2,2]octane (DAPI) or 10 μg/ml propidium iodide. Conventional epifluorescence microscopy was performed with a Zeiss Axiophot microscope. Images were captured with a CCD-1300-Y camera (Princeton Instruments) and processed with Metamorph software (4.5r5 Universal Imaging). Confocal microscopy was performed with a Leica TCS-NT confocal microscope, using a Leica PL APO 100×/1.40-0.70 oil-immersion objective. Optical sections were recorded in 0.4 μm increments using sequential capture of double immunostains.

Caspase assay

Cultured myofibres were fixed in 4% PAF for 5 min and permeabilised for 10 min with 0.1% CHAPS and 2 mM EDTA in Ca^{2+}/Mg^{2+}-free PBS. Myofibres were washed in 2 mM EDTA in Ca^{2+}/Mg^{2+}-free PBS and then incubated with 0.25 mM fluorogenic caspase-8 substrate: rhodamine 110, bis-(*N*-CBZ-L-isoleucyl-L-glutamyl-L-threonyl-L-aspartic acid amide) (Molecular Probes) in 2 mM EDTA in Ca^{2+}/Mg^{2+}-free PBS for 30 min at 37°C. Myofibres were washed in 0.025% Tween20 in PBS, mounted without coverslip in 20% glycerol and viewed immediately on an epifluorescence microscope using a fluorescein filter set. Myofibres were subsequently processed for Pax7 or MyoD immunofluorescence.

TUNEL assay

Cultured myofibres were fixed in 4% PAF for 30 min, washed in PBS and then processed with TACS TdT fluorescein according to the manufacturer's protocols (R&D Systems). Stained myofibres were subsequently processed for Pax7 immunofluorescence.

Cell counting and statistics

The numbers of immunopositive cells per myofibre were counted by varying the focal plane at each point along the myofibre and are shown as the mean value ±SEM. Statistical differences between pairs of samples were assessed by unpaired 2-tailed Student's *t*-test. Statistical differences between multiple samples were assessed by Kruskal–Wallis non-parametric ANOVA with Dunn's post-test (GraphPad InStat 3.0a software).

Results

Localisation of erbB receptors in uninjured skeletal muscle

In sections of C57Bl/10 TA muscles, strong erbB1 immunoreactivity was observed at the neuromuscular junction (NMJ, Fig. 1A), identified by co-staining with α-bungarotoxin (Fig. 1A′). ErbB1 was also present generally on the surface of muscle fibres, connective tissue and capillaries (arrowhead and arrow, respectively in Fig. 1A). In agreement with previous studies [25,26] erbB2, erbB3 and erbB4 receptors were detected at the NMJ (Figs. 1B–D′). ErbB2 and erbB3 were additionally present on vasculature and connective tissues (Figs. 1B, C), in agreement with a previous study in rat [41]. Only erbB4 was present exclusively at NMJs (Fig. 1D′). NRDc was also localised predominantly to the NMJ (Fig. 1E′). However, towards the centre of the NMJ, NRDc immunostaining extended deep to the myofibre by an estimated 3–4 μm (arrowhead in Fig. 1E′). In addition, a subset of muscle fibres exhibited uniform NRDc immunoreactivity (asterisks in Fig. 1E), perhaps indicating differential expression in particular fibre types. In order to determine whether quiescent satellite cells expressed any erbB receptors, we used cryosections of EDL muscles from the $Myf5^{nLacZ/+}$ transgenic mouse, in which β-galactosidase is expressed by quiescent satellite cells [42]. Staining with X-gal identified satellite cell nuclei (blue dye reaction product marked with arrowheads in Figs. 1H–N). Co-immunofluorescence staining revealed that none of the receptors were detectable on quiescent satellite cells (Figs. 1H′–L′). DAPI staining confirmed the location of satellite cell nuclei, although DAPI fluorescence is masked where the X-gal reaction product is particularly intense at the thickest, central region of the nucleus (merged antibody/DAPI shown in Figs. 1H″–L″). Importantly, DAPI can still be detected in a ring at the periphery of the nucleus. Thus, X-gal does not mask any fluorescence from the satellite cell cytoplasm or cell surface, where erbB receptors would be located.

Please cite this article as: J.P. Golding, et al., Skeletal muscle stem cells express anti-apoptotic ErbB receptors during activation from quiescence, Exp. Cell Res. (2006), doi:10.1016/j.yexcr.2006.10.019

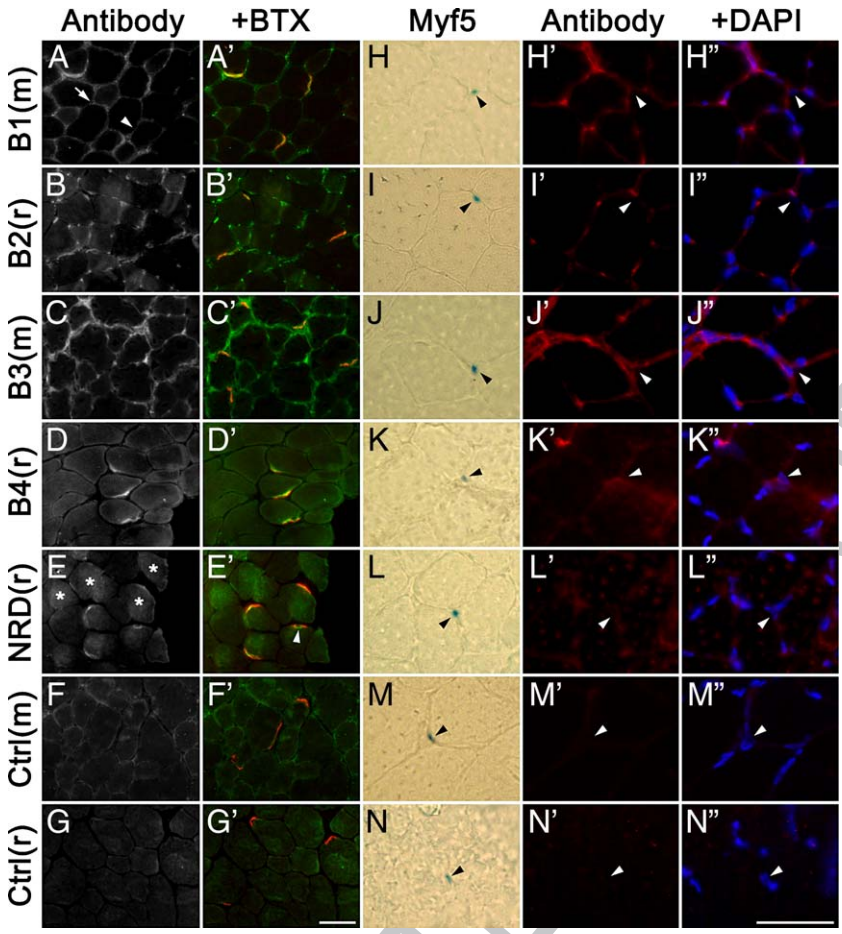

Fig. 1 – ErbB receptor distribution on undamaged panel muscles. (A–G′) C57Bl/10 TA muscle transverse sections were dual stained with receptor-specific antibodies (green in merged images) and α-bungarotoxin to label the NMJ (BTX, red in merged images). Host species of primary antibody is denoted by mouse (m) or rabbit (r) in parenthesis after the antibody name. ErbB1 is present on myofibre surfaces (arrowhead in panel A) and on interstitial tissues and capillaries (arrow in A). (E, E′) NRDc is occasionally present deep to the NMJ (arrowhead in panel E′) and identifies a subset of myofibres (asterisks in E). (H–N″) Myf5$^{nLacZ/+}$ TA muscle transverse sections, triple labelled with (H–N) X-gal to identify Myf5+ satellite cell nuclei; (H′–L′) receptor-specific antibodies; and (H″–N″) merged antibody and DAPI nuclear stain images. Satellite cell nuclei are marked with an arrowhead in each series of images. (F, M′) Ctrl(m) and (G, N′) Ctrl(r) are, respectively, mouse and rabbit IgG controls photographed under identical conditions. Scale bars are 50 μm. (For interpretation of the references to colour in this figure legend, the reader is referred to the web version of this article.)

Localisation of erbB receptors during activation of satellite cells

Isolated EDL myofibre preparations, free of connective tissue, capillaries and other non-muscle cells were maintained in 10% serum-containing medium for between 6 and 48 h. During this period, the satellite cells associated with each myofibre become activated (by the criterion of MyoD expression) and at around 24 h enter into vigorous cell division with a resultant rapid amplification of their myogenic progeny [4,42].

During the earliest stages of activation from quiescence (within the first 6 h), neither MyoD immunoreactivity nor Myf5 expression accurately identify all satellite cells [4,42]. Therefore, to investigate erbB receptor distribution on satellite cells at 6 h in vitro (T6), we used EDL myofibres isolated from the MLC-3F^{nLacZ} transgenic mouse, in which β-galactosidase is expressed exclusively by differentiated myonuclei. This approach allows the identification of all of the associated satellite cells, as they do not express the transgene and therefore fail to stain with X-gal [42] (Figs. 2A–G″. Note that in those cells expressing β-galactosidase the intensely coloured X-gal reaction product masks the underlying DAPI nuclear fluorescence.) Typically, about 8 satellite cells are associated with each EDL myofibre [4]. At T6, erbB1 was detectable on 1.8±0.4 satellite cells per myofibre; about one quarter of the satellite cell population (23/92 of the X-gal-negative cells on 13 fibres ± SEM, Figs. 2A–A‴). ErbB2 was detectable on all satellite cells, with 4.4±0.5 satellite cells per myofibre (about half the population) being strongly immunofluorescent (84/165 of the X-gal-negative cells on 19 fibres ±SEM; strongly erbB2 immunofluorescent cell arrowed; Fig. 2B″). ErbB3 was only weakly detected and was present on 1.4±0.4 satellite cells per myofibre; about 15% of the population (20/132 of the X-gal-negative cells on 14 fibres ±SEM, Fig. 2C). By contrast, erbB4

Please cite this article as: J.P. Golding, et al., Skeletal muscle stem cells express anti-apoptotic ErbB receptors during activation from quiescence, Exp. Cell Res. (2006), doi:10.1016/j.yexcr.2006.10.019

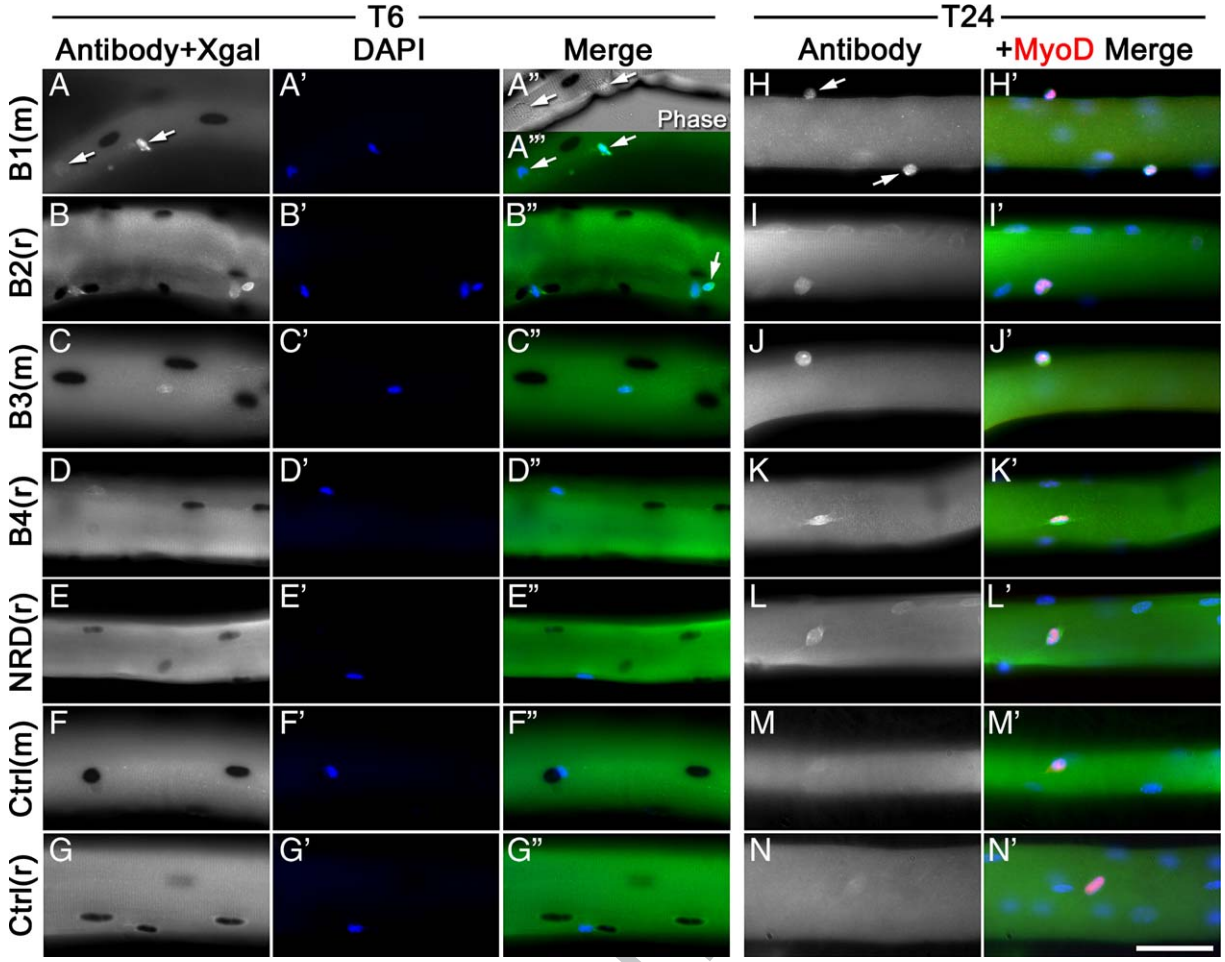

Fig. 2 – Following injury, erbB receptors become localised to activating satellite cells. Isolated EDL myofibres immunostained with receptor-specific antibodies (green in merged images) and DAPI (blue) following 6 or 24 h in 10% serum-containing medium. Host species of primary antibody is denoted by mouse (m) or rabbit (r) in parenthesis after the antibody name. (A–G″) 6 h: MLC-3F^{nLacZ} transgenic myofibres, in which myonuclei stain darkly with X-gal. (A–A″) Approximately 25% of satellite cells show erbB1 immunoreactivity (compare the two arrowed satellite cells). (B–B″) All satellite cells are erbB2 immunopositive, with about half showing strong immunoreactivity (arrowed in B″). (H–N″) 24 h: Myofibres from C57Bl/10 mice. MyoD is red in merged images. (H–H′) ErbB1 immunoreactivity showed variations within the satellite cell population (compare the two cells arrowed in H). (F, M) Ctrl(m) and (G, N) Ctrl(r) are, respectively, mouse and rabbit IgG controls photographed under identical conditions. Scale bar is 50 μm. (For interpretation of the references to colour in this figure legend, the reader is referred to the web version of this article.)

(Fig. 2D) and NRDc (Fig. 2E) were not detected (compare with serum controls in Figs. 2F, G).

After 24 h in vitro, virtually all myofibre-associated satellite cells can be identified by the expression of MyoD [4]. Thus, for experiments at 24 h and later we used EDL myofibres isolated from C57Bl/10 mice, dual stained with MyoD and erbB receptor-specific antibodies.

After 24 h in vitro (T24), erbB1 was detectable on all MyoD+ satellite cells, with intense immunofluorescence observed on 2.9±0.5 satellite cells per myofibre (41/82 MyoD+ cells on 14 fibres ±SEM, compare the intensities of the two satellite cells arrowed in Fig. 2H). All other receptor antibodies demonstrated a uniformity of robust immunofluorescence labelling throughout the MyoD+ satellite cell population. Some MyoD- myonuclei demonstrated weak immunoreactivity with anti-NRDc at T24 (Fig. 2L). Confocal microscopy of T24 myofibres, dual stained with individual anti-erbB antibodies and the nuclear marker propidium iodide, confirmed the surface/cytoplasmic location of erbB1-4 (Figs. 3A–D). Moreover, both confocal microscopy (Figs. 3E, F, O) and conventional epifluorescence microscopy (Figs. 3G–J, K–N, P–S) revealed co-localisation of erbB1/erbB2, erbB2/erbB3 and erbB3/erbB4 in activated satellite cells.

After 48 h in vitro (T48), all myoblasts on isolated mouse EDL myofibres had become strongly immunoreactive for erbB1, erbB2, erbB4 and NRDc, while erbB3 was now only weakly detected (Figs. 4A–E′). After 48 h, myoblasts on isolated myofibres diversify with respect to MyoD expression: a minority reduce their levels of MyoD and return to an undifferentiated quiescent state, while the majority maintain MyoD and eventually express myogenin as they enter terminal differentiation [10]. Importantly, we found that the

Please cite this article as: J.P. Golding, et al., Skeletal muscle stem cells express anti-apoptotic ErbB receptors during activation from quiescence, Exp. Cell Res. (2006), doi:10.1016/j.yexcr.2006.10.019

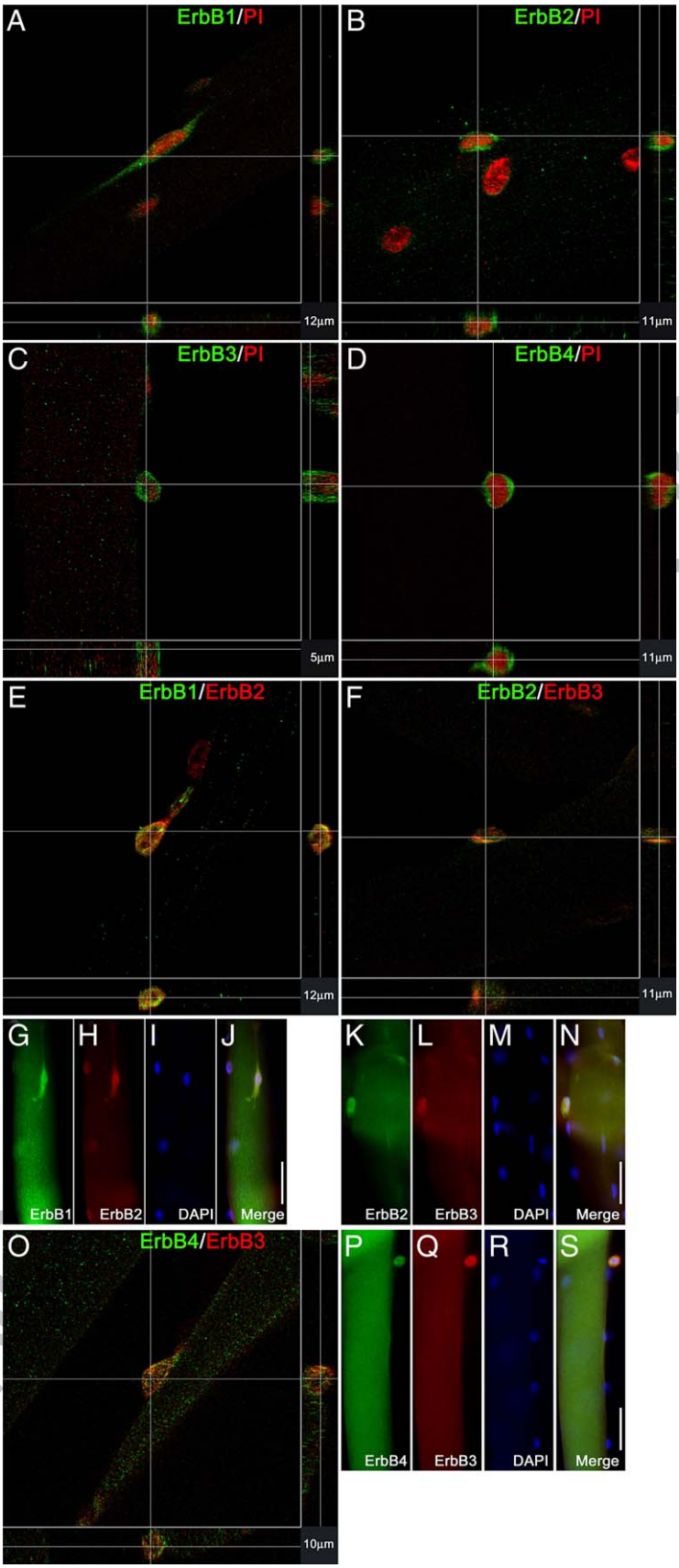

immunofluorescence intensity of erbB receptor and NRDc staining on satellite cells at T48 was equivalent across the entire population, irrespective of variations in MyoD immunoreactivity (in Figs. 4C″, H′, I′ myoblasts showing reduced MyoD staining are marked with arrowheads). However, by T72, the immunofluorescence intensity of erbB2 on isolated EDL

Please cite this article as: J.P. Golding, et al., Skeletal muscle stem cells express anti-apoptotic ErbB receptors during activation from quiescence, Exp. Cell Res. (2006), doi:10.1016/j.yexcr.2006.10.019

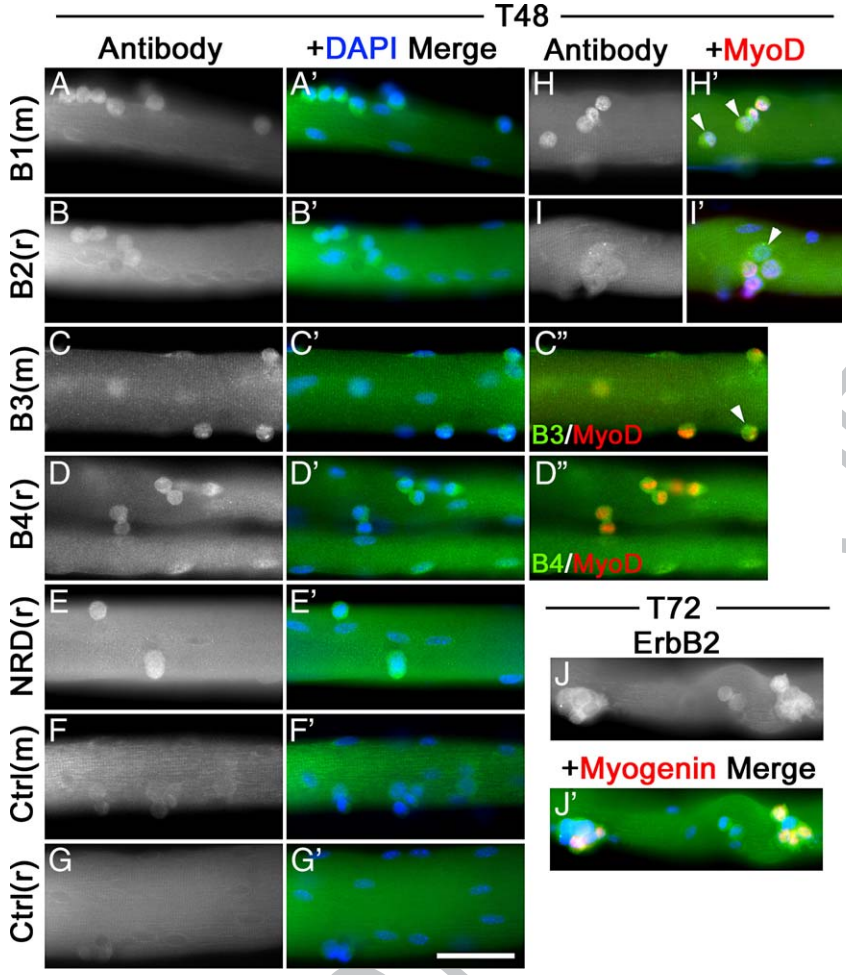

Fig. 4 – Isolated EDL myofibres immunostained following (A–I′) 48 h or (J–J′) 72 h in 10% serum-containing medium with receptor-specific antibodies (green in merged images). Host species of primary antibody is denoted by mouse (m) or rabbit (r) in parenthesis after the antibody name. Arrowheads in (H″, I′ and C′) show a subpopulation of myoblasts labelled with receptor antibodies even when MyoD (red in merged images) is down-regulated. (J–J′) 72 h: ErbB2 immunoreactivity in green and myogenin immunoreactivity in red. (F) Ctrl(m) and (G) Ctrl(r) are, respectively, mouse and rabbit IgG controls photographed under identical conditions. Scale bar is 50 μm. (For interpretation of the references to colour in this figure legend, the reader is referred to the web version of this article.)

myofibres did exhibit variation within the myoblast population (Fig. 4J), being more intense on cells that had committed to differentiation and were co-expressing myogenin (Fig. 4J′).

Not all satellite cells have active erbB receptors

To begin to address what functions erbB receptors might play during satellite cell activation, we first determined if the receptors are functional. ErbB ligand growth factors are present in normal serum [43–45] and should therefore be freely available in our culture medium. EDL myofibre preparations were maintained in vitro for 24 h and then immunostained with antibodies specific to phosphorylated (active) forms of erbB1 and erbB2. On average, 4.5±1.1 cells per myofibre (n=11 fibres) were immunopositive for phosphorylated erbB1 (Figs. 5A, B) and 2.7±0.5 cells per fibre (n=10 fibres) were immunopositive for phosphorylated erbB2 (Figs. 5E, F). The average number of satellite cells on each of these myofibres was determined to be 6.8±0.5 by subsequent Pax7 immunostaining (not shown). As expected, when T24 cultured myofibres were treated with alkaline phosphatase, prior to immunostaining with anti-phosphorylated erbBs, no immunopositive cells were detected (erbB1 control, Figs. 5C, D; erbB2 control, Figs. 5G, H), confirming that these antibodies recognise only the phosphorylated forms of the receptors. Because erbB1 and erbB2 receptors are exclusively detected on all

Fig. 3 – (A–D) Confocal images of C57Bl/10 isolated EDL myofibres after 24 h in 10% serum containing medium, immunostained with erbB receptor-specific antibodies (green channel) and propidium iodide nuclear marker (PI, red channel). (E, F, O) Co-expression of erbB receptors on satellite cells at T24. Each confocal image is a field 100 μm×100 μm square. The z-axis depth of each confocal image in marked in the bottom right corner. (G–N, P–S) Corresponding epifluorescence images of double immunostained myofibres, plus DAPI nuclear stain. Scale bars in epifluorescence images are 50 μm.

Please cite this article as: J.P. Golding, et al., Skeletal muscle stem cells express anti-apoptotic ErbB receptors during activation from quiescence, Exp. Cell Res. (2006), doi:10.1016/j.yexcr.2006.10.019

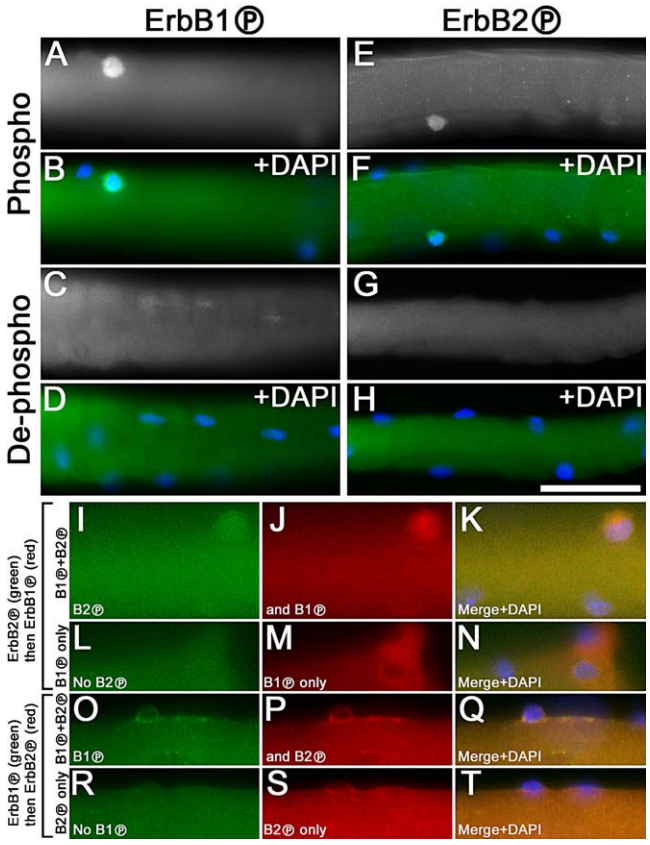

Fig. 5 – (A–H) EDL isolated myofibres cultured for 24 h and immunostained with antibodies specific to (A–D) phosphorylated erbB1 and (E–H) phosphorylated erbB2. (C, D, G, H) Myofibres pre-treated with alkaline phosphatase confirmed the specificity of the antibodies for the phosphorylated forms of the receptors. (I–T) Sequential immunostaining with the anti-phospho antibodies identified cells that contained a mixture of phosphorylated erbB1 and phosphorylated erbB2 (I–K and O–Q), but also cells that had exclusively either (M) phosphorylated erbB1 or (S) phosphorylated erbB2. DAPI counterstaining (blue) identifies cell nuclei. ″=phosphorylated. Scale bar is 50 μm. (For interpretation of the references to colour in this figure legend, the reader is referred to the web version of this article.)

satellite cells by T24 (Fig. 2), this implies that at any one time only about 66% of satellite cells are stimulated via erbB1 and 39% via erbB2 signalling pathways. No pattern was detected in the distribution of these "stimulated" satellite cells along myofibres. In order to help determine whether erbB1 and erbB2 are active in the same cells, we sequentially immunostained T24 myofibres with anti-phospho erbB1 then Alexa 488 secondary antibody, followed by anti-phospho erbB2 then Alexa 594 secondary antibody. Some T24 myofibres were stained in the opposite sequence, i.e., anti-phospho erbB2 was applied first (Figs. 5I–T). We found that 12.9% of labelled cells (4/31 cells on 9 myofibres) labelled exclusively with anti-phospho erbB1 when this was the final layer (compare Figs. 5L and M), while 3.2% of labelled cells (2/63 cells on 16 myofibres) were exclusively anti-phospho erbB2 immunopositive when this was the final layer (compare Figs. 5R and S). Thus, the remaining 83.9% of anti-phospho erbB immunostained cells contain both erbB1 and erbB2 in their phosphorylated forms, corresponding to about three cells per fibre in this experiment.

ErbB ligand growth factors prevent early myoblast cell death

To investigate the consequences of erbB ligand withdrawal, EDL-isolated myofibre preparations were maintained in 10% serum-containing medium for 24 h, to allow up-regulation of erbB receptors on the satellite cells. At this point, the preparations were separated into different culture conditions for a further 24 h (between T24 and T48). Some continued to be maintained in 10% serum medium, while others were washed in DMEM and transferred into serum-free DMEM and supplemented with either: nothing, 1 nM EGF (erbB1 ligand), 1 nM HB-EGF (erbB1,4 and NRDc ligand), 1 nM neuregulin (NRG) (erbB3,4 ligand) or a 1-nM mixture of all three erbB ligand growth factors. Immunostaining confirmed that all erbB receptors and NRDc were still present on myoblasts in preparations deprived of serum between T24 and T48, although the immunofluorescence intensity for erbB1 was reduced (not shown).

As expected, there was a significant difference ($P<0.001$) between the numbers of Pax7+ cells per fibre when comparing serum-maintained with unsupplemented serum-free conditions (compare Figs. 6A and D). Importantly, however, this was not simply attributable to differences in proliferation, since the numbers of Pax7+ cells associated with serum-deprived myofibres was significantly below ($P<0.01$) their starting value on T0 myofibres (Fig. 6G). Supplementation with 1 nM NRG or 1 nM EGF alone similarly resulted in a significant loss of Pax7+ cells compared to T0 ($P<0.01$ and $P<0.001$, respectively; Fig. 6G). By contrast, supplementing serum-free medium with 1 nM HB-EGF or a 1-nM mixture of all three growth factors prevented the loss of Pax7+ cells compared with T0 (Fig. 6G).

A similar trend was seen with MyoD immunoreactivity. Thus, serum-deprived myofibres were associated with significantly fewer MyoD+ cells than serum-maintained controls ($P<0.001$; compare Figs. 6B and E). Supplementing serum-free cultures with a 1-nM mixture of growth factors resulted in a significant increase in the number of MyoD+ cells per fibre compared to serum-free controls ($P<0.001$; Fig. 6G). However, serum-free cultures supplemented with 1 nM NRG or 1 nM EGF had significantly fewer MyoD+ cells per myofibre than cultures supplemented with the growth factor mixture ($P<0.001$ and $P<0.01$, respectively, in Fig. 6G). The number of MyoD+ cells per fibre was statistically indistinguishable between growth factor mixture-supplemented and HB-EGF-supplemented myofibres (Fig. 6G). Although the growth factor mixture increased the number of MyoD+ cells compared to DMEM, or NRG or EGF, it was not as efficient as 10% serum in generating large numbers of MyoD+ cells ($P<0.05$; Fig. 6G).

To assess the role of erbB3 activity in promoting satellite cell survival, a function-blocking concentration of anti-erbB3 antibody (10 μg/ml [46]) was added to serum-maintained myofibre cultures between T24 and T48. Anti-erbB3 had no effect on the numbers of Caspase8+ cells per myofibre (control: 4.25±0.7, $n=12$ myofibres; anti-erbB3: 4.29±0.6, $n=14$ myofibres) but did significantly ($P=0.013$) reduce the number of MyoD+ cells per myofibre from 14.1±1.0 ($n=15$ myofibres) to 10.0±1.2

Please cite this article as: J.P. Golding, et al., Skeletal muscle stem cells express anti-apoptotic ErbB receptors during activation from quiescence, Exp. Cell Res. (2006), doi:10.1016/j.yexcr.2006.10.019

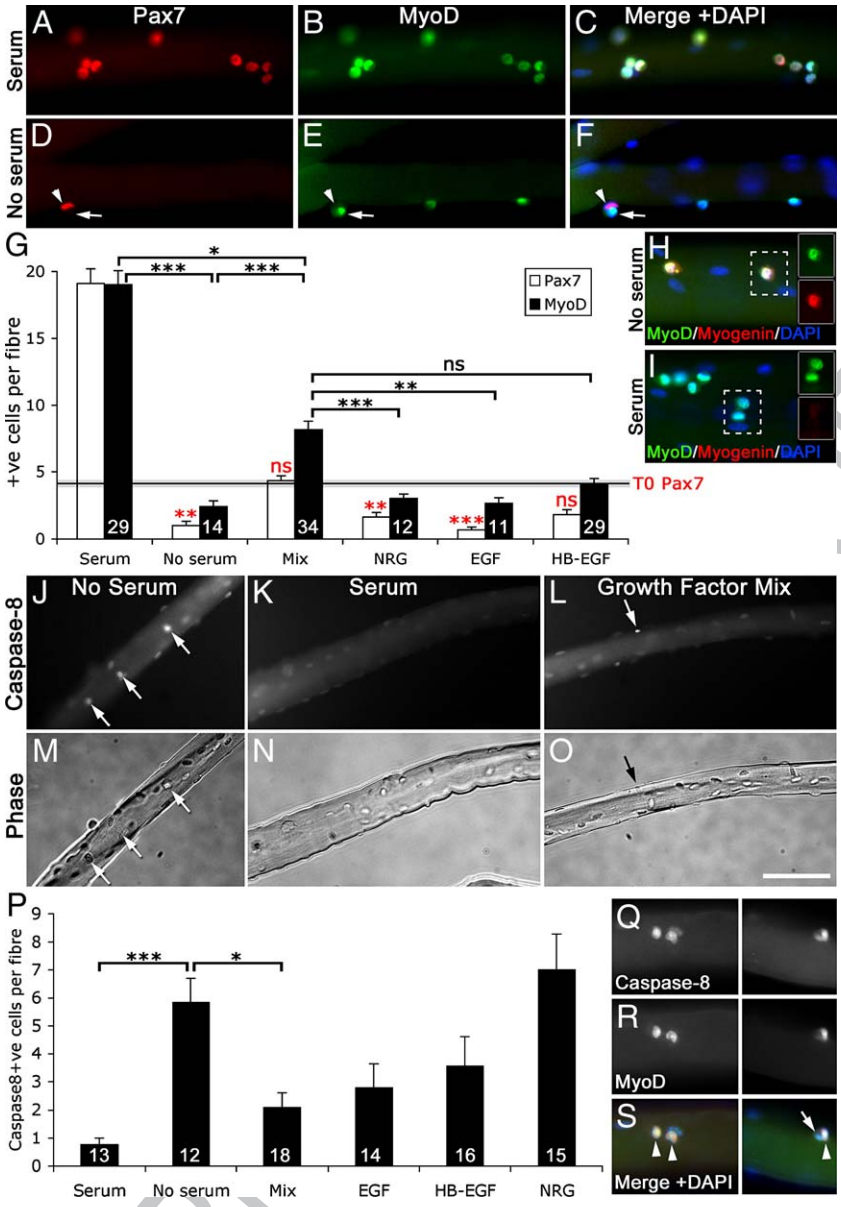

Fig. 6 – ErbB ligand growth factors protect myoblasts from apoptosis. (A–F) Myofibres were maintained in the absence of serum between T24 and T48 and stained for Pax7 (red), MyoD (green) and DAPI (blue). Some cells are returning to quiescence (Pax7+/MyoD– cell identified with arrowhead) and others are differentiating (Pax7–/MyoD+ cell identified with arrow). (G) Comparisons of the mean numbers of Pax7+ and MyoD+ cells per myofibre, on myofibres maintained either in serum, or in serum-free conditions (with or without individual growth factors or a mixture of growth factors). T0 Pax7 indicates the mean number of Pax7+ cells on T0 myofibres. (H, I) Expression of myogenin (red) and MyoD (green) in serum-containing and in serum-free conditions. The fluorescence channels corresponding to the boxed regions in the merged images are shown as separate insets. (J) Many cells activated caspase-8 in serum-free conditions (arrows). (L) Caspase-8 activation was substantially prevented by the mixture of growth factors (arrows), quantified in panel P. (M–O) corresponding phase contrast images. (Q–S) The majority of apoptotic cells were MyoD+ (arrowheads in merged image S). A rare caspase8+/MyoD– exception is arrowed in panel S (inset). DAPI counterstaining (blue) identifies cell nuclei. Scale bar is 100 μm for panels J–O. For all other images, this bar is 50 μm. Statistical analyses: *$P<0.05$, **$P<0.01$, ***$P<0.001$, ns = not significant. (For interpretation of the references to colour in this figure legend, the reader is referred to the web version of this article.)

(*n* = 18 myofibres). Any effects of anti-erbB3 on cell proliferation were not assessed.

As myoblasts withdraw from the cell cycle as a prelude to terminal differentiation, they begin to express myogenin and subsequently down-regulate MyoD. However, differentiation cannot account for the lower numbers of MyoD+ cells upon serum withdrawal. Differentiation was apparent in the preparations maintained from T24 to T48 in serum-free conditions, since 94.4% (51/54) of MyoD+ cells co-expressed myogenin (Fig. 6H). In contrast, no myogenin+ cells (0/162)

Please cite this article as: J.P. Golding, et al., Skeletal muscle stem cells express anti-apoptotic ErbB receptors during activation from quiescence, Exp. Cell Res. (2006), doi:10.1016/j.yexcr.2006.10.019

were present on myofibres maintained in 10% serum (Fig. 6I). Growth factor supplementation had no effect on the proportion of differentiating cells compared to serum-deprived myofibres (1 nM EGF: 92.1% (82 myogenin+/89 MyoD+); 1 nM HB-EGF: 89.8% (53/59); 1 nM NRG: 95.7% (44/46); or a 1-nM growth factor mixture: 97.2% (69/71)). Crucially, no MyoD–/myogenin+ cells were detected on serum-deprived myofibres. This is important because it shows that upon serum deprivation, all the differentiating myogenin+ cells continue to express MyoD. Therefore, the observed reduction in the number of MyoD+ cells must indeed represent a true absence of these cells and not simply a differentiation-induced change of phenotype. An alternative explanation for the loss of MyoD+ cells might be that serum-deprived myoblasts return to their Pax7+/MyoD-quiescent state. However, since the number of Pax7+ cells is also reduced, to significantly less than the T0 value, a return to quiescence can be discounted.

To determine whether apoptotic cell death might account for the loss of MyoD+ cells upon serum deprivation, we assayed myofibre preparations for the activation of caspase-8. Caspase-8 was chosen because it is activated very early during apoptosis, being a critical initiator of the death receptor pathway [47], but additionally regulating the mitochondrial pathway by promoting the activation of Bax and Bak [48]. Furthermore, caspase-8 is activated by singlet oxygen ROS, upstream of caspase-3 activation [49]. In the absence of serum between T24 and T48, six-fold more cells on myofibres activated caspase-8 than in serum-containing control conditions (compare Figs. 6J, M with Figs. 6K, N; quantified in Fig. 6P). The majority of apoptosing caspase-8+ cells on T24–T48 serum-deprived myofibres were also MyoD+ (73.7%, 14/19 cells; Fig. 6S). Conversely, and in agreement with the Pax7/MyoD immunoreactivity data of Fig. 6G, serum-deprived myofibre preparations supplemented with a 1-nM mixture of growth factors demonstrated significantly less caspase-8 activation than serum-deprived controls ($P<0.05$; Figs. 6L, O, P). Serum-deprived preparations supplemented with 1 nM EGF or 1 nM HB-EGF, but not 1 nM NRG alone, also demonstrated reduced caspase-8 activation (Fig. 6P). Although it is clear that apoptosis is initiated in MyoD+ myoblasts in response to serum deprivation (Figs. 6J–S), because caspase-8 activity was only assayed at T48, we cannot formally conclude that apoptosis is the only mechanism by which myoblasts are lost during the T24–T48 period of serum deprivation.

Taken together, these data suggest that a mixture of erbB1/erbB4 ligands (EGF and HB-EGF) but not an erbB3/erbB4 ligand (NRG) act to protect activated satellite cells and their myoblast progeny from cell death.

Inhibition of erbB2 signalling promotes myoblast apoptosis

ErbB1 is the common receptor bound by EGF and HB-EGF, although subsequent signal transduction can occur either via erbB1 homodimers or via erbB1/erbB2 heterodimers [50,51]. To determine whether inhibition of either erbB1 or erbB2 signalling leads to satellite cell or myoblast apoptosis, we examined caspase-8 activity in myofibre preparations cultured for 6 h, 24 h or 48 h in 10% serum-containing medium supplemented with highly specific inhibitors of erbB1 or erbB2 tyrosine phosphorylation: AG1478 and AG825, respectively [37] (Figs. 7A–N). By T24, approximately two times more cells exhibited caspase-8 activity in the presence of AG825 (Figs. 7E, M) compared to either AG1478 (Fig. 7G, M) or unsupplemented controls (Figs. 7H, M). These preparations were subsequently immunostained, revealing that it was predominantly Pax7+ satellite cells that were undergoing apoptosis (arrowheads in Figs. 7B′, F′, J′). Although AG825-induced caspase-8 activation peaked at T24 (Fig. 7M), it took a further 24 h for this initiation of cell death to be reflected in a significant depletion of Pax7+ cells on AG825-treated myofibres (Fig. 7N). Thus, AG825 resulted on average in a loss of one Pax7+ cell per fibre (~15% of the satellite cell population) by T24, and four Pax7+ cells per fibre by T48, compared to unsupplemented controls (Fig. 7N). The erbB inhibitors did not affect satellite cell activation or cell cycle progression. Thus, in separate experiments, Pax7+ satellite cells activated MyoD as normal in the presence of AG825 (T0–T24 AG825: 189 Pax7+/184 MyoD+, $n=26$ fibres. T0–T24 control: 284Pax7+/277 MyoD+, $n=30$ fibres); while 95 of 96 Pax7+ cells incorporated BrdU (from 9 fibres) during 48 h in the continuous presence of AG825 plus BrdU.

The loss of Pax7+ cells in the presence of AG825 appeared modest, although consistent with the values obtained from the serum-free growth factor supplementation experiments (Fig. 6G). To better model the oxidative stresses that myofibres are subjected to immediately following damage in vivo, we maintained myofibres in 10% serum-containing medium for 6 h to allow erbB receptors to become up-regulated (see Fig. 2), and then supplemented half of the myofibre preparations with 100 μM hydrogen peroxide (H_2O_2), with or without erbB inhibitors, for a further 18 h until T24. This concentration of H_2O_2 was chosen because it is high enough to induce a stress response in myofibres but does not affect their viability [52]. The presence of H_2O_2 in itself did not cause a significant loss of Pax7+ cells (Fig. 7O). Only in cultures co-supplemented with H_2O_2 and AG825 or AG1478 were there significant losses of Pax7+ cells (Fig. 7O).

TUNEL provides a sensitive indicator of late-stage apoptotic cells, after DNA fragmentation has occurred. Consistent with the caspase-8 results, exposure of myofibres to AG825 in 10% serum-containing medium for 24 h led to an increase in the proportion of dual TUNEL+/Pax7+ cells per fibre (10.7 ± 4.4%, $n=10$ fibres; Figs. 7P–R), compared to unsupplemented controls (4.6 ± 2.1%, $n=18$ fibres; Figs. 7S–U).

Pro- and anti-apoptotic signals in activating satellite cells

Signal transduction via erbB receptors can activate several distinct intracellular signalling pathways that include phosphatidylinositol 3′ kinase/protein kinase B (PI3-K/Akt), Ras/mitogen-activated protein kinase (Ras/MAP-K) and phospholipase Cγ/protein kinase C (PLCγ/PKC) [22,24]. In addition, erbB2 (via erbB1–erbB2 heterodimers) directly phosphorylates the transcription factor STAT3 [53]. Each of these erbB signal transduction pathways has been implicated in opposing survival and apoptosis decisions within a variety of cell-types, including muscle [54–57]. Therefore, in order to identify the pro-and anti-apoptotic signalling pathways operating in satellite cells during the first 24 h in culture, we examined the effects of inhibitors specific to these various pathways.

Please cite this article as: J.P. Golding, et al., Skeletal muscle stem cells express anti-apoptotic ErbB receptors during activation from quiescence, Exp. Cell Res. (2006), doi:10.1016/j.yexcr.2006.10.019

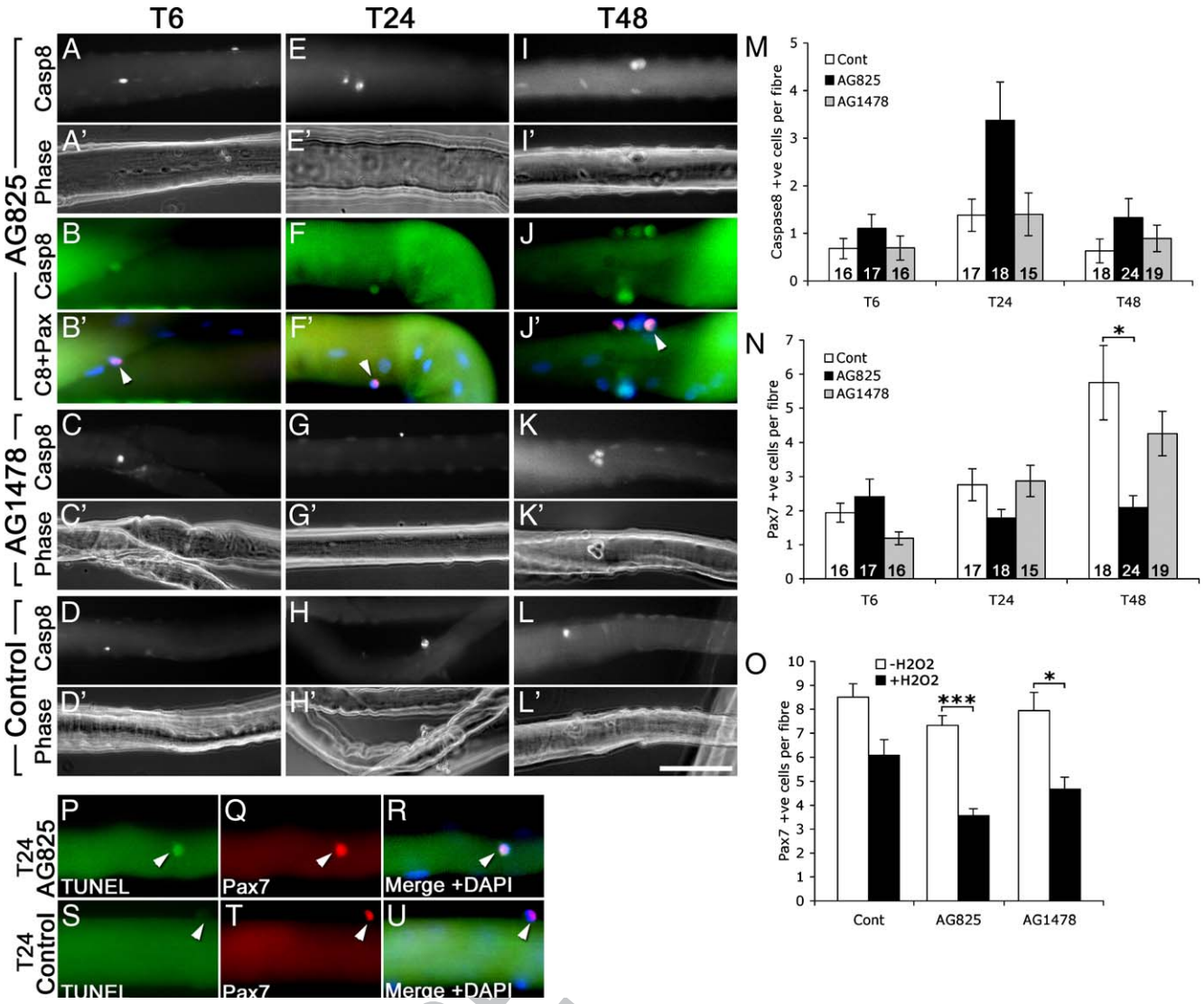

Fig. 7 – Inhibition of erbB2 function leads to satellite cell and myoblast apoptosis. (A–L′) Mouse isolated EDL myofibres show similar levels of caspase-8 activation following 6 h or 48 h exposure to AG825, AG1478 or control conditions. (E–H′) Following 24 h exposure many more cells demonstrate caspase-8 activation in (E) AG825, than in (G) AG1478, or (H) control conditions. (B′, F′, J′) Double caspase-8/Pax7 immunostaining reveals that satellite cells are the predominant apoptosing cell type at each time point (double-positive cells marked with arrowheads). (M) Graphical representation of the caspase-8 data, illustrating the peak of AG825-induced apoptosis at T24. (N) Number of Pax7+ cells per myofibre in the presence of AG825 or AG1478, compared to control. (O) Between T0 and T24, AG825 and AG1478 cause significant losses of Pax7+ satellite cells under conditions of elevated oxidative stress (supplementation with 100 μM H_2O_2). (P–U) Double TUNEL/Pax7 immunostaining confirmed satellite cell apoptosis following 24 h exposure to AG825 (P–R), but not in control conditions (S–U). Statistical analyses: *$P<0.05$, ***$P<0.001$.

EDL myofibres, isolated from the same mouse, were maintained for 24 h in 10% serum-containing medium in the continuous presence of individual inhibitors, with or without AG825, and were then assayed for caspase-8 activity, followed by dual Pax7/MyoD immunostaining. The numbers of immunopositive and caspase-8+ cells were counted on 15–20 myofibres per condition (Fig. 8A). This batch of myofibres had more satellite cells per fibre and was twice as sensitive to AG825 than the group used in Figs. 7A–N; with four-fold more caspase-8+ cells per fibre and an average loss of two Pax7+ satellite cells per fibre following 24 h in AG825, compared with untreated control myofibres (Fig. 8A).

Inhibition of STAT3 resulted in a similar level of caspase-8 activation to that seen following erbB2 inhibition. However, despite this high caspase-8 activity, satellite cell numbers were reduced by on average only one satellite cell per myofibre. Co-inhibition of STAT3 and erbB2 caused hypercontraction of all fibres, precluding further analysis. These data indicate an anti-apoptotic role for the STAT3 pathway during satellite cell activation from quiescence (Fig. 8A).

Inhibition of Akt resulted in an average loss of one satellite cell per fibre, although caspase-8 was not elevated; suggesting a slight protective, although not necessarily anti-apoptotic, role for Akt signalling (Fig. 8A).

Please cite this article as: J.P. Golding, et al., Skeletal muscle stem cells express anti-apoptotic ErbB receptors during activation from quiescence, Exp. Cell Res. (2006), doi:10.1016/j.yexcr.2006.10.019

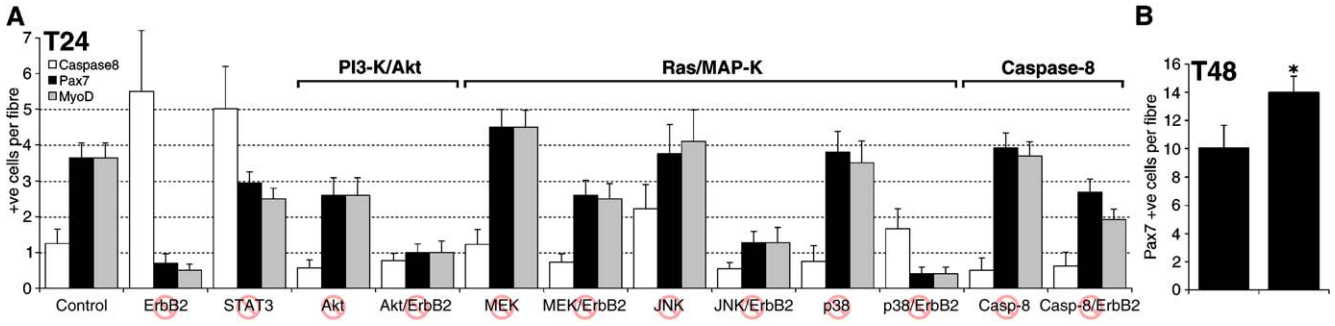

Fig. 8 – (A) Myofibres were exposed to a variety of signal transduction pathway inhibitors for 24 h, in the absence or presence of the erbB2 inhibitor AG825 (inhibited pathways indicated on *x*-axis). The number of caspase-8+, Pax7+ and MyoD+ cells per myofibre were quantified for each condition. (B) Effect of transient inhibition of MEK (between T0 and T24) on the numbers of Pax7+ cells per myofibre at T48. Statistical analyses: *$P<0.05$.

Conversely, inhibition of MEK resulted in a net gain of one satellite cell per fibre compared with controls. Importantly, all satellite cells counted following MEK inhibition were well-isolated singlets, with no evidence of premature cell division compared with the control preparations. Moreover, co-inhibition of MEK and erbB2 partially rescued the loss of satellite cells seen with erbB2 inhibition alone. This would suggest that the Ras/MEK pathway has a net pro-apoptotic effect during satellite cell activation, accounting for a background loss of one satellite cell per fibre by T24 under our relatively benign 10% serum-containing medium culture conditions (Fig. 8A).

Inhibition of JNK or p38 MAP-K pathways had no effect on satellite cell numbers, even though JNK inhibition caused a slight increase in caspase-8 activation (Fig. 8A). Inhibition of PLCγ/PKC caused myofibre hypercontraction within 24 h, preventing any analysis of satellite cells under these conditions.

The control number of satellite cells per fibre was maintained following competitive inhibition of caspase-8. Dual caspase-8/erbB2 co-inhibition partially prevented the loss of satellite cells seen following erbB2 inhibition alone (2.7±0.4 versus 0.7±0.3 Pax7+ cells per fibre, $n=16$ fibres), confirming that satellite cell death following erbB2 inhibition occurs via caspase-8-mediated apoptosis (Fig. 8A).

Inhibition of MEK pro-apoptotic signals improves myoblast survival

We found that by inhibiting Ras/MEK-mediated pro-apoptotic signals in activating satellite cells under our relatively benign culture conditions, we could protect on average one satellite cell per myofibre from apoptosis (~15% of the satellite cell population) (Fig. 8A). We predicted that this modest improvement in satellite cell survival should subsequently be reflected in a proportionate increase in the number of amplifying myoblast progeny. To confirm this, EDL myofibre preparations were maintained in 10% serum-containing medium in the continuous presence of MEK inhibitor plus BrdU for 24 h, during the period of satellite cell activation. The myofibres were then washed and maintained for a further 24 h (until T48) in 10% serum without BrdU or inhibitor. To disassociate any effects of proliferation from survival, some preparations were fixed after the initial 24 h and anti-BrdU immunostaining confirmed that MEK inhibition did not cause premature entry into the cell cycle (both control and MEK-treated myofibres had 1 BrdU+ cell per 10 myofibres). Pax7 immunostaining revealed that temporary inhibition of MEK between T0 and T24 significantly increased ($P<0.05$) the average number of myoblasts per myofibre that survived to T48 (14 cells/fibre, $n=19$ fibres), compared to controls (10 cells/fibre, $n=20$ fibres; Fig. 8B). From our knowledge of satellite cell proliferation kinetics in vitro [4], two cell doublings should have occurred by T48. Thus, the extra four myoblasts per fibre is fully consistent with the protection of on average one satellite cell per myofibre during the activation phase.

Discussion

Previous studies have reported that erbB2, erbB3 and erbB4 receptors are expressed by normal adult skeletal muscles exclusively at the NMJ [25,26], while erbB1–erbB3 receptors have been detected on differentiating myoblasts in vitro [21,31–33]. However, the expression of erbB receptors by myogenic cells during the intervening period, at the onset of muscle regeneration, has hitherto not been explored. Here, we provide the first description that erbB1-4 receptor tyrosine kinases and NRDc co-receptor become expressed by satellite cells, the stem cell population of adult skeletal muscle, as they activate from quiescence. Signals transduced via erbB receptors control a diverse set of cellular functions, from growth, migration and differentiation, to survival and apoptosis [22]. Within myoblasts, the functions attributed to erbB signalling include neuregulin/erbB3-mediated promotion of differentiation and fusion [33] and erbB2-dependent survival of differentiating myoblasts [21]. Specifically, erbB2 conditional knockout mice have been created, in which the muscle creatine kinase promoter (MCK) drives Cre-mediated excision of floxed erbB2 exclusively in heart and skeletal muscles [21]. These erbB2-deficient mice exhibit extensive myoblast apoptosis during differentiation [21]. However, MCK is not expressed by undifferentiated satellite cells [58] and only becomes expressed during myoblast differentiation [21], so the role of erbB2 during the early stages of muscle regeneration could not be assessed in that model.

Using the isolated myofibre culture system, an in vitro model of satellite cell activation, we have found that although

Please cite this article as: J.P. Golding, et al., Skeletal muscle stem cells express anti-apoptotic ErbB receptors during activation from quiescence, Exp. Cell Res. (2006), doi:10.1016/j.yexcr.2006.10.019

absent during quiescence, erbB receptors can be detected on satellite cells after 6 h of culture under activating conditions. This is well before cell division occurs in this model system [10] and so erbB signalling cannot play a significant role in cell proliferation or differentiation at this stage. Instead, our results suggest that signalling via erbB2, and to a lesser extent via erbB1, provides an anti-apoptotic survival mechanism for satellite cells undergoing activation; a process that normally occurs in the context of a damaged, degenerating muscle environment. Sequential staining experiments indicate that erbB1 and erbB2 are phosphorylated co-ordinately in >80% of satellite cells at T24, although this may not necessarily be in the form of erbB1/erbB2 heterodimers. It is unclear what functions erbB3 and erbB4 might serve in activated satellite cells. Canto et al. [29,59] show that erbB3 and erbB4 signalling are important for glucose transport in skeletal muscle, although it is not known whether satellite cells are involved. We found that inhibition of erbB3 between T24 and T48 did not promote caspase-8-mediated apoptosis, although the number of MyoD+ cells was lower than controls, suggesting a possible role in promoting cell proliferation or a return to quiescence. The role of erbB4 signalling is not explored directly in this paper. ErbB4 is detectable from T24 onwards on satellite cells and it could be operating in the form of erbB4/erbB2 heterodimers. However, it is clear that NRG, an important erbB4 ligand, is insufficient by itself to promote satellite cell survival even though it was used at a concentration (71 ng/ml) that should maximise receptor stimulation (ED_{50} 0.5–2.0 ng/ml, R&D Systems data sheet).

In serum-free conditions, a mixture of three erbB ligands (NRG, EGF and HB-EGF) was found to reduce caspase-8 activation in myoblasts and to help preserve myoblast cell numbers, although it remains to be proven if this link is causal. These erbB ligands were specifically chosen because they are produced by skeletal muscle [60–62], and it is therefore likely that these growth factors would be readily available to satellite cells following myotrauma. Despite the likely availability of erbB ligand growth factors, only a subpopulation of satellite cells were found to be using erbB1 or erbB2 signalling at any one time during activation. Thus, by T24, about 3 satellite cells per myofibre robustly express erbB1 and have the receptor in a phosphorylated state; while all satellite cells express erbB2 by T24, although only about 2 satellite cells per myofibre have erbB2 in a phosphorylated state. These values are consistent with our observation that between T0 and T24 about one satellite cell per myofibre (~15% of the quiescent population) is protected from apoptosis by erbB2 signalling. In the presence of increased oxidative stress (100 μM H_2O_2), a closer analogy to in vivo myotrauma and ischemia-reperfusion injuries [12–14,19,63], an additional two satellite cells per myofibre (~45% of the population) are protected from cell death by erbB2 signalling.

In a variety of cell types, ROS stimulates erbB1 phosphorylation [64,65], and because erbB1 activation can transactivate erbB2 [22,66,67], it follows that those satellite cells under the greatest pro-apoptotic stress should exhibit the highest activity of erbB1/erbB2. If the anti-apoptotic signals are removed, by inhibiting erbB2 phosphorylation using AG825, then these cells become overwhelmed by pro-apoptotic signals and die.

The pro-apoptotic and anti-apoptotic mechanisms that operate in activating satellite cells are most likely complex and interactive. Nevertheless, erbB signalling modules are well placed to be important master regulators of these signalling networks. Thus, erbB receptor signalling directly activates Ras/Raf/MAP-K, PI3-K/Akt, PLCγ/PKC and STAT signal transduction pathways. All of these root pathways can subsequently affect the survival/apoptosis balance of the cell, although the details are cell-type dependent and sometimes contradictory [54]. Moreover, the apoptotic process can feed back on erbB signalling, since several caspases cleave erbB1 and erbB2 [54,68].

Our data indicate an anti-apoptotic role for STAT3 within activating satellite cells. STAT3 becomes potently activated in satellite cells within 3 h of myotrauma [69] and induces the transcription of anti-apoptotic Bcl-2/x and caspase inhibitors [54], the latter being consistent with our observation of a large increase in caspase-8 activation following STAT3 inhibition. Because erbB1–erbB2 heterodimers directly phosphorylate STAT3 [53], any erbB1/2 signalling is likely to provide a crucial source of phosphorylated STAT3 to help maintain the viability of a stressed satellite cell.

Conversely, our data suggest a pro-apoptotic role for MEK within activating satellite cells. Little is known concerning the role of MEK in apoptosis, although interestingly one report demonstrates that inhibition of MEK1,2 prevents apoptosis in a lung cancer cell line [70]. We find that inhibition of MEK1,2 phosphorylation preserves on average one satellite cell per myofibre, subsequently resulting in a proportionate increase in the numbers of proliferating myoblast progeny. Co-inhibition of MEK and erbB2 prevents the loss of satellite cells normally seen with erbB2 inhibition alone. The different outcomes of MEK inhibition and MEK/erbB2 dual-inhibition would be consistent with a model whereby erbB2 signals act to prevent apoptosis initiation, while MEK signals promote apoptosis execution. Although our data suggests direct intracellular links between erbB1/2 signalling and apoptotic pathways in satellite cells, we cannot exclude the possibility that erbB1/2 activation initiates a cascade of extracellular signalling between satellite cells and the parent myofibre that then indirectly leads to the initiation of apoptosis within the satellite cell. For instance, cleavage of erbB2 by caspase-8 in MCF7 cancer cells results in their increased susceptibility to the pro-apoptotic inflammatory cytokine TNF-α [68,71], also expressed within muscle following reperfusion injury [72].

From a therapeutic perspective, our data suggest that inhibitors of erbB2 activity, such as the anti-cancer drug Herceptin, may have unforeseen adverse effects on skeletal muscle regeneration; while prompt and acute inhibition of MEK following muscle damage could protect at least 15% of satellite cells from cell death, thereby increasing the overall efficiency of adult skeletal muscle regeneration. These results may also have relevance both for muscle wasting diseases such as cachexia [73]; and for muscular dystrophy, characterised by repeated rounds of muscle degeneration and regeneration.

Acknowledgments

We thank Peter Zammit for comments on the manuscript. This work was funded by the MRC and by the MYORES Network of Excellence (contract 511978) from the European

Please cite this article as: J.P. Golding, et al., Skeletal muscle stem cells express anti-apoptotic ErbB receptors during activation from quiescence, Exp. Cell Res. (2006), doi:10.1016/j.yexcr.2006.10.019

Commission 6th Framework Programme. JPG is funded by an MRC Collaborative Career Development Fellowship in Stem Cell Research.

REFERENCES

[1] A. Mauro, Satellite cell of skeletal muscle fibers, J. Biophys. Biochem. Cytol. 9 (1961) 493–495.

[2] F.P. Moss, C.P. Leblond, Satellite cells as the source of nuclei in muscles of growing rats, Anat. Rec. 170 (1971) 421–435.

[3] C.A. Collins, I. Olsen, P.S. Zammit, L. Heslop, A. Petrie, T.A. Partridge, J.E. Morgan, Stem cell function, self-renewal, and behavioral heterogeneity of cells from the adult muscle satellite cell niche, Cell 122 (2005) 289–301.

[4] P.S. Zammit, L. Heslop, V. Hudon, J.D. Rosenblatt, S. Tajbakhsh, M.E. Buckingham, J.R. Beauchamp, T.A. Partridge, Kinetics of myoblast proliferation show that resident satellite cells are competent to fully regenerate skeletal muscle fibers, Exp. Cell Res. 281 (2002) 39–49.

[5] S.S. Jejurikar, W.M. Kuzon Jr., Satellite cell depletion in degenerative skeletal muscle, Apoptosis 8 (2003) 573–578.

[6] P.M. Siu, E.E. Pistilli, D.C. Butler, S.E. Alway, Aging influences cellular and molecular responses of apoptosis to skeletal muscle unloading, Am. J. Physiol.: Cell Physiol. 288 (2005) C338–C349.

[7] M.C. Kamradt, F. Chen, S. Sam, V.L. Cryns, The small heat shock protein alpha B-crystallin negatively regulates apoptosis during myogenic differentiation by inhibiting caspase-3 activation, J. Biol. Chem. 277 (2002) 38731–38736.

[8] K. Dee, M. Freer, Y. Mei, C.M. Weyman, Apoptosis coincident with the differentiation of skeletal myoblasts is delayed by caspase 3 inhibition and abrogated by MEK-independent constitutive Ras signaling, Cell Death Differ. 9 (2002) 209–218.

[9] Z. Yablonka-Reuveni, A.J. Rivera, Temporal expression of regulatory and structural muscle proteins during myogenesis of satellite cells on isolated adult rat fibers, Dev. Biol. 164 (1994) 588–603.

[10] P.S. Zammit, J.P. Golding, Y. Nagata, V. Hudon, T.A. Partridge, J.R. Beauchamp, Muscle satellite cells adopt divergent fates: A mechanism for self-renewal? J. Cell Biol. 166 (2004) 347–357.

[11] A.C. Wozniak, J. Kong, E. Bock, O. Pilipowicz, J.E. Anderson, Signaling satellite-cell activation in skeletal muscle: markers, models, stretch, and potential alternate pathways, Muscle Nerve 31 (2005) 283–300.

[12] L. Zuo, T.L. Clanton, Reactive oxygen formation in the transition to hypoxia in skeletal muscle, Am. J. Physiol.: Cell Physiol. (2005).

[13] M. Stangel, U.K. Zettl, E. Mix, J. Zielasek, K.V. Toyka, H.P. Hartung, R. Gold, H2O2 and nitric oxide-mediated oxidative stress induce apoptosis in rat skeletal muscle myoblasts, J. Neuropathol. Exp. Neurol. 55 (1996) 36–43.

[14] V. Adams, S. Gielen, R. Hambrecht, G. Schuler, Apoptosis in skeletal muscle, Front. Biosci. 6 (2001) D1–D11.

[15] M. Benhar, D. Engelberg, A. Levitzki, ROS, stress-activated kinases and stress signaling in cancer, EMBO Rep. 3 (2002) 420–425.

[16] D. Caporossi, S.A. Ciafre, M. Pittaluga, I. Savini, M.G. Farace, Cellular responses to H(2)O(2) and bleomycin-induced oxidative stress in L6C5 rat myoblasts, Free Radical Biol. Med. 35 (2003) 1355–1364.

[17] V. Renault, L.E. Thornell, G. Butler-Browne, V. Mouly, Human skeletal muscle satellite cells: aging, oxidative stress and the mitotic clock, Exp. Gerontol. 37 (2002) 1229–1236.

[18] S. Fulle, S. Di Donna, C. Puglielli, T. Pietrangelo, S. Beccafico, R. Bellomo, F. Protasi, G. Fano, Age-dependent imbalance of the antioxidative system in human satellite cells, Exp. Gerontol. 40 (2005) 189–197.

[19] L.L. Ji, C. Leeuwenburgh, S. Leichtweis, M. Gore, R. Fiebig, J. Hollander, J. Bejma, Oxidative stress and aging. Role of exercise and its influences on antioxidant systems, Ann. N. Y. Acad. Sci. 854 (1998) 102–117.

[20] M. Horikawa, S. Higashiyama, S. Nomura, Y. Kitamura, M. Ishikawa, N. Taniguchi, Upregulation of endogenous heparin-binding EGF-like growth factor and its role as a survival factor in skeletal myotubes, FEBS Lett. 459 (1999) 100–104.

[21] E.R. Andrechek, W.R. Hardy, A.A. Girgis-Gabardo, R.L. Perry, R. Butler, F.L. Graham, R.C. Kahn, M.A. Rudnicki, W.J. Muller, ErbB2 is required for muscle spindle and myoblast cell survival, Mol. Cell. Biol. 22 (2002) 4714–4722.

[22] T. Holbro, N.E. Hynes, ErbB receptors: directing key signaling networks throughout life, Annu. Rev. Pharmacol. Toxicol. 44 (2004) 195–217.

[23] E. Nishi, A. Prat, V. Hospital, K. Elenius, M. Klagsbrun, N-arginine dibasic convertase is a specific receptor for heparin-binding EGF-like growth factor that mediates cell migration, EMBO J. 20 (2001) 3342–3350.

[24] M.D. Marmor, K. Bose Skaria, Y. Yarden, Signal transduction and oncogenesis by ErbB/HER receptors, Int. J. Radiat. Oncol. Biol. Phys. 58 (2004) 903–913.

[25] X. Zhu, C. Lai, S. Thomas, S.J. Burden, Neuregulin receptors, erbB3 and erbB4, are localized at neuromuscular synapses, EMBO J. 14 (1995) 5842–5848.

[26] J.C. Trinidad, G.D. Fischbach, J.B. Cohen, The Agrin/MuSK signaling pathway is spatially segregated from the Neuregulin/ErbB receptor signaling pathway at the neuromuscular junction, J. Neurosci. 20 (2000) 8762–8770.

[27] S.A. Jo, X. Zhu, M.A. Marchionni, S.J. Burden, Neuregulins are concentrated at nerve-muscle synapses and activate ACh-receptor gene expression, Nature 373 (1995) 158–161.

[28] N. Altiok, J.L. Bessereau, J.P. Changeux, ErbB3 and ErbB2/neu mediate the effect of heregulin on acetylcholine receptor gene expression in muscle: differential expression at the endplate, Embo J. 14 (1995) 4258–4266.

[29] C. Canto, E. Suarez, J.M. Lizcano, E. Grino, P.R. Shepherd, L.G. Fryer, D. Carling, J. Bertran, M. Palacin, A. Zorzano, A. Guma, Neuregulin signaling on glucose transport in muscle cells, J. Biol. Chem. 279 (2004) 12260–12268.

[30] P. Fumagalli, M. Accarino, A. Egeo, P. Scartezzini, G. Rappazzo, A. Pizzuti, V. Avvantaggiato, A. Simeone, G. Arrigo, O. Zuffardi, S. Ottolenghi, R. Taramelli, Human NRD convertase: a highly conserved metalloendopeptidase expressed at specific sites during development and in adult tissues, Genomics 47 (1998) 238–245.

[31] B.D. Ford, B. Han, G.D. Fischbach, Differentiation-dependent regulation of skeletal myogenesis by neuregulin-1, Biochem. Biophys. Res. Commun. 306 (2003) 276–281.

[32] J.M. Harper, P.J. Buttery, Effects of EGF receptor ligands on fetal ovine myoblasts, Domest. Anim. Endocrinol. 20 (2001) 21–35.

[33] D. Kim, S. Chi, K.H. Lee, S. Rhee, Y.K. Kwon, C.H. Chung, H. Kwon, M.S. Kang, Neuregulin stimulates myogenic differentiation in an autocrine manner, J. Biol. Chem. 274 (1999) 15395–15400.

[34] R. Kelly, S. Alonso, S. Tajbakhsh, G. Cossu, M. Buckingham, Myosin light chain 3F regulatory sequences confer regionalized cardiac and skeletal muscle expression in transgenic mice, J. Cell Biol. 129 (1995) 383–396.

[35] S. Tajbakhsh, E. Bober, C. Babinet, S. Pournin, H. Arnold, M. Buckingham, Gene targeting the myf-5 locus with nlacZ reveals expression of this myogenic factor in mature skeletal muscle fibres as well as early embryonic muscle, Dev. Dyn. 206 (1996) 291–300.

[36] J.D. Rosenblatt, A.I. Lunt, D.J. Parry, T.A. Partridge, Culturing

Please cite this article as: J.P. Golding, et al., Skeletal muscle stem cells express anti-apoptotic ErbB receptors during activation from quiescence, Exp. Cell Res. (2006), doi:10.1016/j.yexcr.2006.10.019

satellite cells from living single muscle fiber explants, In Vitro Cell Dev. Biol., Anim. 31 (1995) 773–779.
[37] A. Levitzki, A. Gazit, Tyrosine kinase inhibition: an approach to drug development, Science 267 (1995) 1782–1788.
[38] N. Osherov, A. Gazit, C. Gilon, A. Levitzki, Selective inhibition of the epidermal growth factor and HER2/neu receptors by tyrophostins, J. Biol. Chem. 268 (1993) 11134–11142.
[39] E. Hamada, T. Nishida, Y. Uchiyama, J. Nakamura, K. Isahara, H. Kazuo, T.P. Huang, T. Momoi, T. Ito, H. Matsuda, Activation of Kupffer cells and caspase-3 involved in rat hepatocyte apoptosis induced by endotoxin, J. Hepatol. 30 (1999) 807–818.
[40] J. Turkson, D. Ryan, J.S. Kim, Y. Zhang, Z. Chen, E. Haura, A. Laudano, S. Sebti, A.D. Hamilton, R. Jove, Phosphotyrosyl peptides block Stat3-mediated DNA binding activity, gene regulation, and cell transformation, J. Biol. Chem. 276 (2001) 45443–45455.
[41] N.K. Lebrasseur, G.M. Cote, T.A. Miller, R.A. Fielding, D.B. Sawyer, Regulation of neuregulin/ErbB signaling by contractile activity in skeletal muscle, Am. J. Physiol.: Cell Physiol. 284 (2003) C1149–C1155.
[42] J.R. Beauchamp, L. Heslop, D.S. Yu, S. Tajbakhsh, R.G. Kelly, A. Wernig, M.E. Buckingham, T.A. Partridge, P.S. Zammit, Expression of CD34 and Myf5 defines the majority of quiescent adult skeletal muscle satellite cells, J. Cell Biol. 151 (2000) 1221–1234.
[43] T. Joh, M. Itoh, K. Katsumi, Y. Yokoyama, T. Takeuchi, T. Kato, Y. Wada, R. Tanaka, Physiological concentrations of human epidermal growth factor in biological fluids: use of a sensitive enzyme immunoassay, Clin. Chim. Acta 158 (1986) 81–90.
[44] S. Chakrabarty, S. Huang, T.L. Moskal, H.A. Fritsche Jr., Elevated serum levels of transforming growth factor-alpha in breast cancer patients, Cancer Lett. 79 (1994) 157–160.
[45] S.E. Bastian, A.J. Dunbar, I.K. Priebe, P.C. Owens, C. Goddard, Measurement of betacellulin levels in bovine serum, colostrum and milk, J. Endocrinol. 168 (2001) 203–212.
[46] L.M. Gilmour, K.G. Macleod, A. McCaig, J.M. Sewell, W.J. Gullick, J.F. Smyth, S.P. Langdon, Neuregulin expression, function, and signaling in human ovarian cancer cells, Clin. Cancer Res. 8 (2002) 3933–3942.
[47] M. Kruidering, G.I. Evan, Caspase-8 in apoptosis: the beginning of "the end"? IUBMB Life 50 (2000) 85–90.
[48] S.H. Kaufmann, M.O. Hengartner, Programmed cell death: alive and well in the new millennium, Trends Cell Biol. 11 (2001) 526–534.
[49] S. Zhuang, M.C. Lynch, I.E. Kochevar, Caspase-8 mediates caspase-3 activation and cytochrome c release during singlet oxygen-induced apoptosis of HL-60 cells, Exp. Cell Res. 250 (1999) 203–212.
[50] D.S. Lidke, P. Nagy, R. Heintzmann, D.J. Arndt-Jovin, J.N. Post, H.E. Grecco, E.A. Jares-Erijman, T.M. Jovin, Quantum dot ligands provide new insights into erbB/HER receptor-mediated signal transduction, Nat. Biotechnol. 22 (2004) 198–203.
[51] D. Graus-Porta, R.R. Beerli, J.M. Daly, N.E. Hynes, ErbB-2, the preferred heterodimerization partner of all ErbB receptors, is a mediator of lateral signaling, EMBO J. 16 (1997) 1647–1655.
[52] F. McArdle, S. Spiers, H. Aldemir, A. Vasilaki, A. Beaver, L. Iwanejko, A. McArdle, M.J. Jackson, Preconditioning of skeletal muscle against contraction-induced damage: the role of adaptations to oxidants in mice, J. Physiol. 561 (2004) 233–244.
[53] A. Fernandes, A.W. Hamburger, B.I. Gerwin, ErbB-2 kinase is required for constitutive stat 3 activation in malignant human lung epithelial cells, Int. J. Cancer 83 (1999) 564–570.
[54] A.J. Danielsen, N.J. Maihle, The EGF/ErbB receptor family and apoptosis, Growth Factors 20 (2002) 1–15.
[55] X. Liu, K. Ye, Src homology domains in phospholipase C-gamma1 mediate its anti-apoptotic action through regulating the enzymatic activity, J. Neurochem. 93 (2005) 892–898.
[56] X.T. Wang, K.D. McCullough, X.J. Wang, G. Carpenter, N.J. Holbrook, Oxidative stress-induced phospholipase C-gamma 1 activation enhances cell survival, J. Biol. Chem. 276 (2001) 28364–28371.
[57] T. Mutoh, T. Kumano, H. Nakagawa, M. Kuriyama, Role of tyrosine phosphorylation of phospholipase C gamma1 in the signaling pathway of HMG-CoA reductase inhibitor-induced cell death of L6 myoblasts, FEBS Lett. 446 (1999) 91–94.
[58] G. Ferrari, G. Salvatori, C. Rossi, G. Cossu, F. Mavilio, A retroviral vector containing a muscle-specific enhancer drives gene expression only in differentiated muscle fibers, Hum. Gene Ther. 6 (1995) 733–742.
[59] C. Canto, A.V. Chibalin, B.R. Barnes, S. Glund, E. Suarez, J.W. Ryder, M. Palacin, J.R. Zierath, A. Zorzano, A. Guma, Neuregulins mediate calcium-induced glucose transport during muscle contraction, J. Biol. Chem. 281 (2006) 21690–21697.
[60] J.A. Abraham, D. Damm, A. Bajardi, J. Miller, M. Klagsbrun, R.A. Ezekowitz, Heparin-binding EGF-like growth factor: characterization of rat and mouse cDNA clones, protein domain conservation across species, and transcript expression in tissues, Biochem. Biophys. Res. Commun. 190 (1993) 125–133.
[61] L. Frati, G. Cenci, G. Sbaraglia, D.V. Teti, I. Covelli, Levels of epidermal growth factor in mice: tissues measured by a specific radioreceptor assay, Life Sci. 18 (1976) 905–911.
[62] M. Hiramatsu, M. Kashimata, F. Takayama, K. Tsubakida, K. Ri, N. Minami, Reduced level of epidermal growth factor in the skeletal muscle of mice with muscular dystrophy, Horm. Metab. Res. 24 (1992) 138–139.
[63] B.B. Rubin, G. Chang, S. Liauw, A. Young, A. Romaschin, P.M. Walker, Phospholipid peroxidation deacylation and remodeling in postischemic skeletal muscle, Am. J. Physiol. 263 (1992) H1695–H1702.
[64] Y. Fang, S.I. Han, C. Mitchell, S. Gupta, E. Studer, S. Grant, P.B. Hylemon, P. Dent, Bile acids induce mitochondrial ROS, which promote activation of receptor tyrosine kinases and signaling pathways in rat hepatocytes, Hepatology 40 (2004) 961–971.
[65] K. Takeyama, K. Dabbagh, J. Jeong Shim, T. Dao-Pick, I.F. Ueki, J.A. Nadel, Oxidative stress causes mucin synthesis via transactivation of epidermal growth factor receptor: role of neutrophils, J. Immunol. 164 (2000) 1546–1552.
[66] R. Goldman, R.B. Levy, E. Peles, Y. Yarden, Heterodimerization of the erbB-1 and erbB-2 receptors in human breast carcinoma cells: a mechanism for receptor transregulation, Biochemistry 29 (1990) 11024–11028.
[67] C.R. King, I. Borrello, F. Bellot, P. Comoglio, J. Schlessinger, Egf binding to its receptor triggers a rapid tyrosine phosphorylation of the erbB-2 protein in the mammary tumor cell line SK-BR-3, EMBO J. 7 (1988) 1647–1651.
[68] V. Benoit, A. Chariot, L. Delacroix, V. Deregowski, N. Jacobs, M.P. Merville, V. Bours, Caspase-8-dependent HER-2 cleavage in response to tumor necrosis factor alpha stimulation is counteracted by nuclear factor kappaB through c-FLIP-L expression, Cancer Res. 64 (2004) 2684–2691.
[69] K. Kami, E. Senba, In vivo activation of STAT3 signaling in satellite cells and myofibers in regenerating rat skeletal muscles, J. Histochem. Cytochem. 50 (2002) 1579–1589.
[70] T.T. Nguyen, E. Tran, T.H. Nguyen, P.T. Do, T.H. Huynh, H. Huynh, The role of activated MEK-ERK pathway in quercetin-induced growth inhibition and apoptosis in A549 lung cancer cells, Carcinogenesis 25 (2004) 647–659.

Please cite this article as: J.P. Golding, et al., Skeletal muscle stem cells express anti-apoptotic ErbB receptors during activation from quiescence, Exp. Cell Res. (2006), doi:10.1016/j.yexcr.2006.10.019

[71] S.S. Jejurikar, E.A. Henkelman, P.S. Cederna, C.L. Marcelo, M.G. Urbanchek, W.M. Kuzon Jr., Aging increases the susceptibility of skeletal muscle derived satellite cells to apoptosis, Exp. Gerontol. (2006).
[72] F. Zhang, E.C. Hu, J. Gerzenshtein, M.P. Lei, W.C. Lineaweaver, The expression of proinflammatory cytokines in the rat muscle flap with ischemia-reperfusion injury, Ann. Plast. Surg. 54 (2005) 313–317.
[73] J.E. Belizario, M.J. Lorite, M.J. Tisdale, Cleavage of caspases-1, -3, -6, -8 and -9 substrates by proteases in skeletal muscles from mice undergoing cancer cachexia, Br. J. Cancer 84 (2001) 1135–1140.

Please cite this article as: J.P. Golding, et al., Skeletal muscle stem cells express anti-apoptotic ErbB receptors during activation from quiescence, Exp. Cell Res. (2006), doi:10.1016/j.yexcr.2006.10.019